Conference Proceedings

Solar World Congress 2015
Daegu, Korea, 08 – 12 November 2015

SPANISH RENEWABLE ENERGY GENERATION SHORT-TERM FORECAST

Nicolas Perez-Mora[1,2], Victor Martinez-Moll[2] and Vincent Canals [2]

[1] SAMPOL Ingeniería y Obras, Palma of Majorca (Spain)

[2] University of Balearic Islands, Palma of Majorca (Spain)

Abstract

This work presents and compare four short-term forecasting methods for one day-ahead hourly values of Spanish solar and wind energy generation. From the four models analyzed, two are based on ARIMAX statistical methods and the other two are based on computational intelligence methods as Non-linear Autoregressive eXogenous Neural Networks (NARX). Both forecasting methodologies use the same numerical weather prediction data (NWP), consisting for solar energy, on solar irradiation and for wind power, on wind speed. The NWP data is combined in the model with the installed power of the different generation technologies in Spain. In addition to the NWP data, the models are fed with the aggregated solar and wind energy generation in hourly steps provided by the Spanish Transport System Operator (TSO).

The obtained results by the forecasting methods and by the different energy generation technologies are compared using different error metrics such as: MBE, RMSE, MAE, MAPE and MADPE.

Keywords: *Forecasting, Solar Irradiation, Solar Forecasting, Wind Forecasting, Energy Market, ARIMAX, Neural Networks, NARX, Time Series*

1. Introduction

A huge number of renewable energy power plants have been installed in the previous decade. This was due the subsidies promoting the construction of green power plants (Monteiro et al., 2013b) and the increase in the price of fossil fuels. These factors became a huge boost for the renewable energy generation, being the installation of renewables a profitable business (Monteiro et al., 2013a). Such expansion and the policies adopted by many countries to integrate renewables into the energy generation mix has brought a rearrangement of the energy market (Rubin and Babcock, 2013).

The integration of energy generated by green power plants into electric power system is priority, meaning that this power is fed into the system in preferential order within the energy mix. Although the volatility and variability of the renewable resource makes the integration in the grid difficult taking into account that the supply and load of electric power must be balanced at every instant.

In the Spanish Energy Market or Pool the total electricity power production is balanced in hour step with the demand. The electricity is traded in different markets: the main market “daily” (D) and the 6 regulation markets “intra-daily” (ID). In the daily market the producers release their bids at 12:00 for next day’s hourly generation. The intra daily markets take place: at 17:00 for ID1, at 21:00 for ID2, at 01:00 for ID3, at 04:00 for ID4, at 08:00 for ID5, at 12:00 for ID6; the generators can release their bids covering each hour from a few hour after the auction time till the end of the auctioned day, as long as that bid modifies a previous bid placed in the daily market.

The energy mix is the result of the counter clockwise auctions where the demand and the cheapest combination of generation energies matches. The retribution for all the accepted generators in an hour will be the same and equal to the last and highest accepted bid in the auction. In order to always ensure the renewable energy

doi:10.18086/swc.2015.07.10 Available at http://proceedings.ises.org

acceptance into the generation mix the green energies place their bids at the legal minimum, 0€/MWh and its retribution would be calculated as the sum of the final auction price times the generated energy plus the generation subsidy stipulated by the government. Such situation brings variations on energy generation prices. Energy generators can increase their profit by matching their production with the high price hours (Perez-Mora et al., 2016). On the other hand, the grid operator may penalize the generator in case that the energy generation is different than the offered in the auction by charging the cost of the deviated energy.

A major drawback for technologies harvesting electricity out from volatile resources is the non-continuous availability of the resource. Solar energy depends critically on the variability of irradiance (Y. Gala et al., 2014), typically cloud cover cause rapid changes in the irradiance during the day (Chen et al., 2011) which brings along generation fluctuations. In the same way, wind energy generation depends on the wind direction, speed and its variations (Cassola and Burlando, 2012). This dependence on weather conditions may lead to wrong or inaccurate bids from the generators in the energy auction and therefore into a penalties from the grid operator. An accurate bid would therefore minimize the penalties. Wind and solar generators might pursue low penalties by relying on energy forecasts (Lange and Focken, 2006; Mahoney et al., 2012; Yang et al., 2012).

This paper presents two different approaches to forecasting for each technology. The first method is based on AutoRegressive Integrated Moving Average (ARIMA) supported with eXplanatory variable (ARIMAX) and other is based on Artificial Neural Networks (ANN), in particular, based on Nonlinear AutoRegressive models with eXogenous Neural Network (NARX). Both methods are proved to provide accurate energy resource forecasts, either through computational models as in ANN (Li and Shi, 2010; Qazi et al., 2015; Reikard, 2009) or using autoregressive models such as ARIMA (Erdem and Shi, 2011; Huang et al., 2012; Paulescu et al., 2013).

This paper is organized as follows: Next section provides an overview of the problem to approach. Section 3 describes the obtained data to use. In Section 4 the methodology used to approach the problem is explained. Section 5 presents the result obtained from the methodology and the conclusions from those is given in Section 6.

2. Problem description

The aim of this work is to propose a comparison between two sets of methods forecasting solar and wind power. Both of the methods are improved with a valid explanatory variable obtained from a Numerical Weather Prediction method (NWP). This comparison is carried out within a specific boundaries conditions such as Spanish Energy market abovementioned, in particular, the forecasts focus on the daily market being the forecast horizon from +12h to +36h in hourly step.

The importance on forecasting green energy generation lies in the variability along the time and markedly different generation potential between stations and different months of the year. In case of solar power it changes from a 540 MW minimum power peak in winter to a 5.6 GW maximum power peak in summer which implies the 12% of the total generation power injected into the grid. For wind power it varies from a minimum of 120 MW to a maximum of 16.9 GW reaching peaks of production which implies the 69.4% of the total injected power into the grid. Wind power does not necessarily follow the seasons per se, but it is possible to see an annual trend line. In 2014 wind power was the resource with the biggest share in the energy mix, 20.9%. The maximum injection power achieved by solar and wind into the grid reached a total of 19.4 GW.

It is important to bear in mind that the solar electricity generation in Spain includes two technologies: photovoltaic with an installed capacity of 4.16GW; and solar thermal power stations with an installed capacity of 2.3GW, additionally these power plants may have with a storage system.

Regarding wind power the main difficulty is the lack of information on wind farm layouts impeding the use of wind direction to estimate the power decrease due shadowing between wind turbines.

A common approach to the forecast problem over a wide region is to calculate individual forecast and sum the results up (Mellit and Pavan, 2010), and it is expectable that individual errors to partially cancel out when summing up the forecasts and thus, obtaining a more accurate prediction (Y. Gala et al., 2014). An aggregated forecast approach for a country like Spain it is an extremely complicated proceeding due the large amount of installations, the variety of technologies and the lack of historical generation information from each generator. Thereby, the approach given in this paper is forecasting the aggregated power for the Spanish peninsular market for each technology. To do so, the forecast methods are supported with a valid explanatory variable which comprises a time series of hourly values.

The mentioned explanatory variables are obtained developing a NWP method. This method provides the cloudiness index and the wind speed for a certain location. In the case of wind power, the wind speed is presumed to be a sufficient and valid explanatory variable. In the other hand solar power, is related with irradiation on the collector surface, thus cloudiness index is inversely correlated with the solar generation. The cloudiness index is a useful information that helps modeling solar irradiation. A model has been developed based on the extraterrestrial radiation modified by the cloudiness index of each location. The obtained value is expected to have a high correlation to the actual irradiation of a given location (Biga and Rosa, 1980; Lorenz et al., 2009).

2.1. Forecasted Irradiation

In order to obtain the irradiation with the developed method it is required to calculate the extraterrestrial hourly radiation (G_0) for a given point (Duffie and Beckman, 2013).This calculation depends upon the location of the plant, the time of the year and the slope of the solar collectors. The radiation (G_0) is calculated according to (eq. 1):

$$G_0 = G_{SC}\left(1 + 0.033\,cos\frac{360n}{365}\right)cos\,\theta_z \qquad \text{(eq. 1)}$$

Where G_{SC} is a solar constant (1367 W/m^2), n is the day number of the year, θ_z is the zenith angle calculated in (eq. 2):

$$cos\,\theta_z = cos(\emptyset - \alpha)\,cos\,\delta\,cos\,\omega + sin(\emptyset - \alpha)\,sin\,\delta \qquad \text{(eq. 2)}$$

The latitude of the location is denoted by $\emptyset$, a is the slope of the collecting surface, δ is the declination or angular position of the sun calculated in (eq. 3) and ω is the hour angle or the angle of displacement of the sun calculated in (eq. 4).

$$\delta = 23.45\,sin\left(360\,\frac{284+n}{365}\right) \qquad \text{(eq. 3)}$$

$$\omega = (h_s - 12)\cdot 15 \qquad \text{(eq. 4)}$$

The solar time is denoted by h_s. The difference between the solar time and the standard time is calculated through the formula (eq. 5) and the result is given in minutes:

$$Solar\ time - standard\ time = 4(L_{st} - L_{loc}) + E + DLS \qquad \text{(eq. 5)}$$

Where L_{st} and L_{loc} are the longitudes for the standard meridian and the location, DLS references the possibility of having Day Light Savings and E is a value calculated through (eq. 6):

$$E = 229.2(0.000075 + 0.001868\cdot cos(B) - 0.032077\cdot sin(B) - 0.014615\,cos(2B) - 0.04089\cdot sin(2B) \qquad \text{(eq. 6)}$$

And finally, B is calculated according (eq. 7):

$$B = (n-1)\frac{360}{365} \qquad \text{(eq. 7)}$$

The intensity of the solar resource that reaches the surface of the earth decreases with increasing values of cloudiness index or sky cover (Sharma et al., 2011). Taking this hypothesis as valid the method forecasts the irradiation (I_f) for a given location as dependent on the extraterrestrial hourly radiation (G_0) and the symmetrical of the forecasted cloudiness measured in 0 to 1 range (N_f). The values are calculated hourly according to (eq. 8):

$$I_f = G_0\cdot(1 - N_f) \qquad \text{(eq. 8)}$$

A similar model was presented by (Zhang et al., 2014), where global irradiance is obtained adding to the model the clouds transmissivity.

2.2. Forecasted wind speed

As mentioned before the wind speed and direction are directly related with the availability of a wind turbine to generate power. In the case of wind direction it could be useful to understand how the wind turbines shadow each other on a wind farm (Astariz et al., 2015; Sørensen et al., 2002), in order to improve the calculation of the explanatory variable. To do so, the wind farms turbine distribution is required, unfortunately this information is not easily accessible. Therefore the only contribution to the explanatory variable is the wind speed in the location. In (eq. 9) the power delivered by a wind turbine is given by (eq. 9):

$$P = \frac{1}{2} \cdot \rho \cdot A \cdot v^3 \qquad \text{(eq. 9)}$$

Where ρ is the air density, A is the area swept by the rotor and v is the wind speed through the blades.

2.3. Weighted explanatory variable

The value of the weighted explanatory variable used for Spain is calculated taking into account the forecasted time series, either irradiation or wind speed, in the measured places and the installed powers in those places. Spain irradiation (I_E) values are calculated according to (eq. 10):

$$I_E = \frac{1}{P_S} \sum_{n=1}^{50} I_{fn} \cdot P_{sn} \qquad \text{(eq. 10)}$$

Where I_{fn} is the forecasted irradiation on the n location, P_{sn} is the installed solar power for a given location, Ps is the total solar power accumulated in Spain and is calculated using (eq. 11).

$$P_S = \sum_{n=1}^{50} P_{sn} \qquad \text{(eq. 11)}$$

Spain wind speed (v_E) values are calculated according to (eq. 12):

$$v_E = \frac{1}{P_w} \sum_{n=1}^{50} v_{fn} \cdot P_{wn} \qquad \text{(eq. 12)}$$

Where v_{fn} is the forecasted wind speed on the n location, P_{wn} is the installed wind power for a given location, P_w is the total wind power accumulated in Spain and is calculated using (eq. 13).

$$P_w = \sum_{n=1}^{50} P_{wn} \qquad \text{(eq. 13)}$$

3. Data acquisition

The required data for both forecasting methods comprises two related time series, the aggregated energy generation and the explanatory variable. The historical data is obtained from the Spanish TSO, *Red Eléctrica de España* (REE). This solar generation data is available from 24/7/2013 and provides the time series of the national solar production in 10min step. In the other hand, wind generation is available from 1/1/2012 and provides the time series of national wind production in 10min step.

The installed power for solar and wind technologies is given by the Ministry of Industry. Detailed information of the installations, such as, location, technology, power and whether or not is connected to grid is provided. This information is processed and clustered according to the province division in Spain. In this way 50 aggregated installed powers are obtained. In the case of solar power, photovoltaic and solar thermal technologies are summed up in each region.

The NWP is based on an algorithm that analyses satellite images and predicts the climatic data (Zhang et al., 2014). The NWP data comprises three days ahead time span. The cloudiness and wind speed database starts on 8/9/2014. In order to have a homogeneous database in the area of Spain, one station per province is used; those stations are located, mainly, in the province's main city, therefore 50 stations are selected for Spain. Stations are marked with black dots in Fig.1.

Fig. 1. Weather Stations Localizations

3.1. Possible source of errors

The variable grid used that takes as unit the provinces may lead into errors since the obtained NWP value is given for a point and it is used in the whole area regardless of either station or the power plant location. The asymmetry in the location of weather stations and the different shapes and sizes of the provinces avoid the possibility of spatial averaging of the NWP data used in (Lorenz et al., 2009) and only the aggregation of the weighted data in the whole country is carried out in this study.

The sum of photovoltaic and solar thermal power plants regardless of the different technologies comprising this categories may lead to errors while forecasting the final output.

The shadowing effect within wind farms due the location of the wind turbines in the land and the wind direction may bring power decreases in the local wind generation and thus affecting the aggregated generation.

For the extraterrestrial hourly radiation calculation a value of slope (α) is estimated, this value is fixed for all the solar power plants and during the year. The most common slope value for Spain is fixed at the average latitude value, 40º. The optimum yearly slope value for an installation could have been taken as the same as the latitude where it is located (Benghanem, 2011).

3.2. Time series correlation

The resulting acquired data gives two pairs of time series, one for solar forecasting and the other for wind forecasting. In order to study the rightness of the abovementioned suppositions two correlation studies have been carried out on the time series, Pearson correlation study and R^2 correlation study.

The results for solar, where irradiation and national solar generation are taken into consideration shows a good correlation (Fig.2a), with a Pearson factor of 0.90 and $R^2 = 0.816$.

The results for wind, where wind speed and national wind generation are taken into consideration shows a correlation (Fig.2b), with a Pearson factor of 0.79 and $R^2 = 0.63$. In the wind speed case the same study is made for wind speed to the power of three (cubic wind speed, v^3) since as seen in (eq. 9) it is related with wind power. This study gives as Pearson factor a result of 0.73 and $R^2 = 0.54$; which is lower than the previous one and thus, simple wind speed is used to forecast.

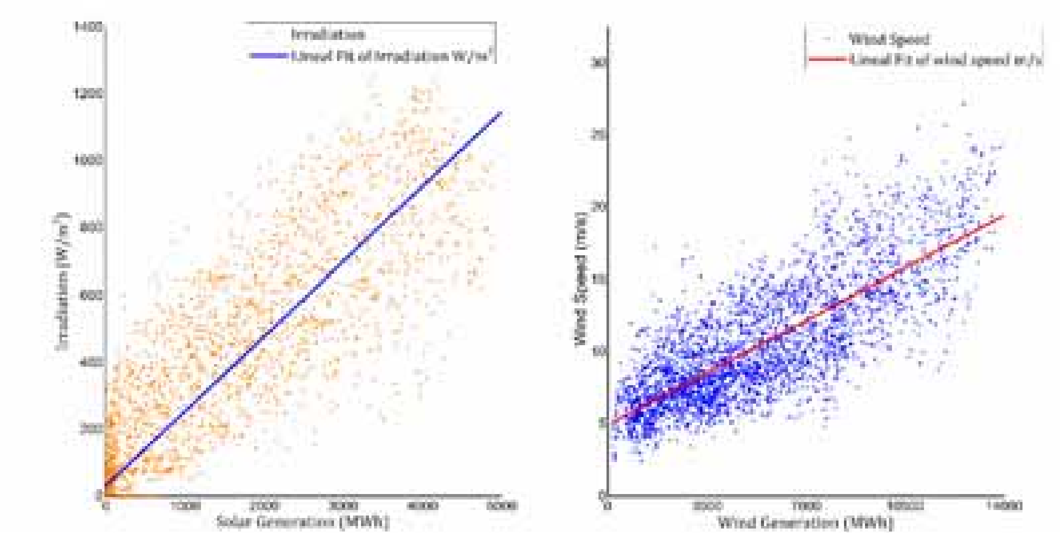

Fig. 2. Variables relation for (a) Solar Generation Vs Irradiation and (b) Wind Generation Vs Wind Speed.

4. Methodology

The relations between the explanatory variables and the generations are reasons to think that the likeness between the time series would be sufficient to calculate the aggregated energy generation (Fig. 3). Nevertheless the relation is not perfect, and in the case of wind is far to be close to 1, adding this to the variability and differences between the various installed power plants, technologies and performances precludes a reliable analytical model. Therefore a statistical forecasting method needs to be developed to obtain the aggregated power hourly generated in Spain.

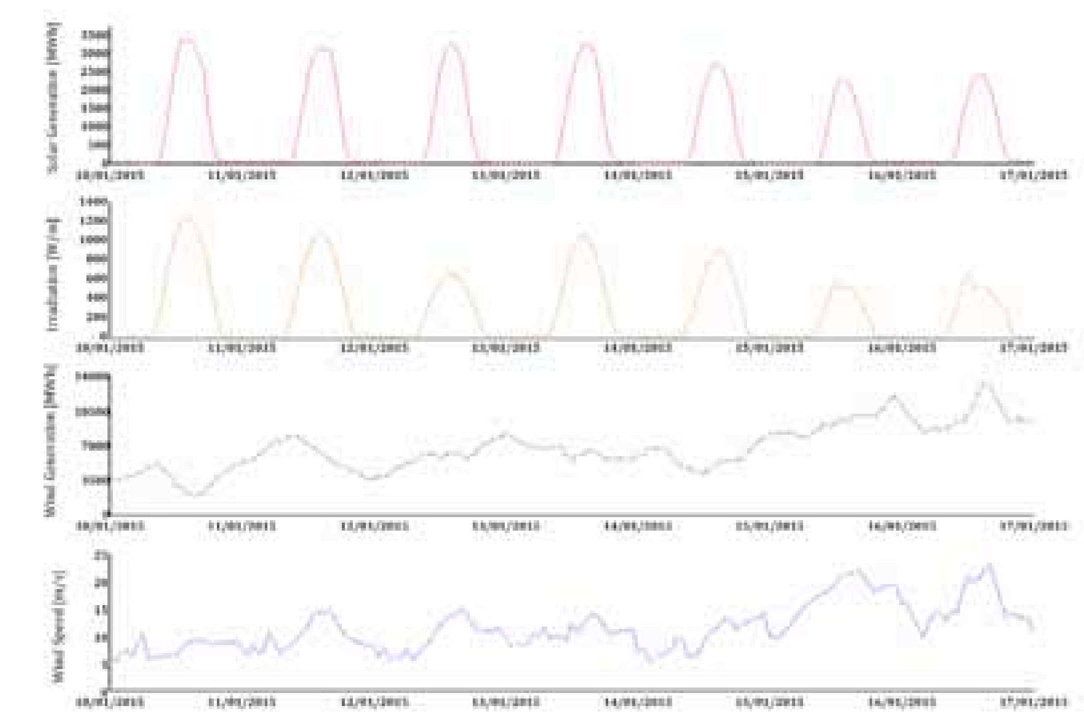

Fig. 3. Generation and proposed explanatory variables

This statistical model is fitted to time series data in order to forecast an extra time series to understand better and predict future values of the main time series. It is composed by an autoregressive model (p), moving average model (q) and differencing degree (D). Mathematically, it can be expressed as: ARIMA (p, D, q).

An approach to the forecast problem is given by the ARIMAX model. This model has been commonly used for forecasting renewable energy resources. Total irradiation is forecasted in (Dong et al., 2013; Reikard, 2009) and wind speed is forecasted in (Erdem and Shi, 2011; Liu et al., 2013).

The other proposed approach to the problem is using neural networks, these are found to outperform the regressions models when it comes to high resolutions (Reikard, 2009). Since the late 1990s ANN have been applied in energy forecasting using climatological variables as inputs to an ANN to predict generation values (Sulaiman et al., 2009). There are several ANN models that approach forecasting, in this work a NARX model is selected since they outperform other ANN models as MLP (Perez-Mora et al., 2015).

NARX model relates the current value of a time series to current and past values of the exogenous series influencing, therefore the series of interest (Da Silva Fonseca et al., 2012). This approach based on ANN which allow to find next values in a time series using past measurements of aggregated power and explanatory variable used as inputs to an autoregressive model with exogenous input (ARX) building therefore a NARX recurrent neural networks.

5. Results

Several combinations and configurations of ARIMAX and NARX models have been tried out to obtain the most accurate results. The configuration of each model is different for each energy source. Nevertheless the length of the time series is the same for both sources, starting on 8/9/14 and finishing on the forecasted days, 17/1/15. The days selected to forecast are a week in January which is the end of the available data set and has changes on weather conditions (cloud cover and wind speed) to evaluate the goodness of the obtained results. The parameters that achieve the best set of results are shown in this section.

For ARIMA forecasting the data is split in training set, 95%; and result comparison set, 5%. The length of the vector in the best performing configurations are shown in Tab. 1; where "MA", stands for vector of non-seasonal moving average coefficients; "SMA", stands for vector of seasonal moving average coefficients corresponding to an invertible polynomial; "AR", stands for vector of non-seasonal autoregressive coefficients; "SAR", stands for vector of seasonal autoregressive coefficients corresponding to a stable polynomial; and "D", stands for integer indicating the degree of the non-seasonal differencing in the time series.

Tab. 1. ARIMA Configurations & Models

NN Method	MA	SMA	AR	SAR	D	Explanatory Variable
ARIMA Solar	3	0	5	0	0	Irradiation
ARIMA Wind	12	5	7	6	0	Wind speed

For NARX forecasting and in order to avoid over fitting, the data is split in training, 70%; validation, 15%; and result comparison and testing, 15%. The training method used in both cases is Levenberg-Marquardt back-propagation algorithm. The results obtained with the configurations are evaluated using the error measurements explain in this chapter. The best performing methods and neural network configurations are shown in Tab. 2; where "L", stands for Linear; "ST", stands for Sigmoid Tangent and "I" stands for Input layer.

Tab. 2. NARX Configurations & Models

NN Method	Number of layers	Neurons in each layer	Activation function	Explanatory Variable
NARX Solar	3	48-24-1	I-ST-L	Irradiation
NARX Wind	3	48-24-1	I-ST-L	Wind speed

The obtained results with the abovementioned methods are presented as an hourly time series of 168 values (equivalent to one week) in Fig. 4 and compared with the real generation.

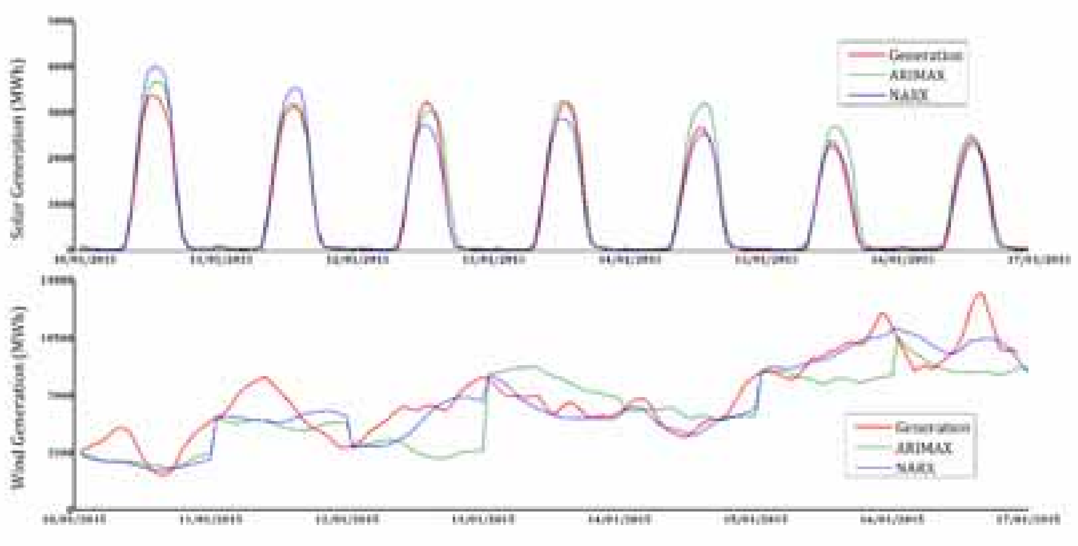

Fig. 4. Different forecast methods results comparison

In order to measure the accuracy of the predictions, the error between the forecasted values and real data is analyzed in this section. To validate the forecast methods in this work, the following calculations are used:

- Mean Bias Error (MBE), shows the deviation of the forecast divided by the installed power. This gives a perception of how the forecasted values are greater or lower than the real ones in percentage (eq. 14).
- Root Mean Square Error (RMSE), shows the deviation of the forecast divided by the installed power. With this error is possible to understand the deviation of the forecast in percentage (eq. 15).
- Mean Absolute Error (MAE), shows the absolute deviation of the forecast divided by the installed power. This gives a perception of the accuracy of the method in terms of percentage (eq. 16), this method is particularly useful for market deviations.
- Mean Absolute Percentage Error (MAPE), shows the same error divided by hourly generation; representing a percentage (eq. 17) (Tseng et al., 2002). This figure is useful to understand the accuracy of the forecast method. The percentage of error escalates when the value of generation is close to zero.
- Mean Daily Absolute Percentage Error (MADPE), the sum of the daily MAE is divided by the sum of the daily generation; thus represents a relative daily error (eq. 18). This figure is useful to understand the accuracy of the method in daily basis, solving MAPE's drawback when generation is close to zero.

$$MBE = \frac{100}{P_{ins}}\frac{1}{n}\sum_{t=1}^{n} S_{(t)} - F_{(t)} \qquad [\%] \qquad \text{(eq. 14)}$$

$$RMSE = \frac{100}{P_{ins}}\sqrt{\frac{1}{n}\sum_{t=1}^{n}\left(S_{(t)} - F_{(t)}\right)^2} \qquad [\%] \qquad \text{(eq. 15)}$$

$$MAE = \frac{100}{P_{ins}}\frac{1}{n}\sum_{t=1}^{n}\left|S_{(t)} - F_{(t)}\right| \quad [\%] \qquad \text{(eq. 16)}$$

$$MAPE = \frac{100}{n}\sum_{t=1}^{n}\left|\frac{S_{(t)}-F_{(t)}}{S_{(t)}}\right| \quad [\%] \qquad \text{(eq. 17)}$$

$$MADPE = \frac{100}{n}\sum_{d=1}^{n}\frac{\sum_{t=1}^{24}\left|S_{(t)}-F_{(t)}\right|}{\sum_{t=1}^{24}\left|S_{(t)}\right|} \quad [\%] \qquad \text{(eq. 18)}$$

As presented before an ARIMA and NARX models for solar and wind energy generation for one day-ahead forecast have been developed. Both of the proposed models accepts as inputs either the hourly irradiation or the wind speed. The output are 24 hourly values of, either, the solar generation or the wind generation in Spain. After several simulations for the four proposed methods the best configuration found gives the results shown in Tab. 3 for the representative weeks evaluated (10/1/15 – 17/1/15).

Tab. 3: Results for ARIMA and NARX models forecasting solar and wind energy generation

	Error	10/1/15	11/1/15	12/1/15	13/1/15	14/1/15	15/1/15	16/1/15	Mean
ARIMAX SOLAR	MBE	1.8%	0.5%	0.8%	0.2%	2.8%	2.8%	0.2%	1.3%
	RMSE	2.8%	1.5%	3.4%	2.0%	4.5%	5.3%	1.7%	3.0%
	MAE	1.8%	1.0%	1.9%	1.2%	2.8%	2.9%	1.2%	1.8%
	MAPE	33.0%	32.9%	44.7%	20.5%	34.3%	51.6%	40.8%	36.8%
	MADPE	12.1%	7.3%	14.5%	8.9%	24.9%	32.7%	11.4%	**16.0%**
ARIMAX WIND	MBE	-3.9%	-3.7%	-10.3%	6.4%	-0.4%	-6.4%	-5.7%	-3.4%
	RMSE	5.4%	7.0%	11.9%	6.8%	4.9%	8.7%	9.4%	7.7%
	MAE	4.6%	6.0%	10.3%	6.4%	3.9%	6.9%	6.9%	6.4%
	MAPE	25.3%	21.9%	36.2%	23.4%	15.2%	15.4%	14.3%	21.7%
	MADPE	27.4%	22.5%	39.1%	22.9%	15.0%	16.7%	15.7%	**22.8%**
NARX SOLAR	MBE	2.6%	1.7%	-1.2%	-1.1%	-0.3%	0.8%	-1.0%	**0.2%**
	RMSE	4.8%	3.1%	3.2%	3.4%	1.4%	1.4%	2.1%	**2.8%**
	MAE	2.8%	2.1%	1.8%	2.1%	0.9%	0.9%	1.5%	**1.7%**
	MAPE	22.2%	32.5%	32.3%	36.9%	44.3%	43.7%	41.7%	36.3%
	MADPE	18.3%	14.6%	13.8%	15.1%	8.3%	10.5%	14.0%	**13.5%**
NARX WIND	MBE	-4.4%	-1.8%	-3.4%	-0.8%	-2.1%	-0.4%	-0.3%	-1.9%
	RMSE	5.9%	7.1%	4.6%	2.1%	3.5%	2.3%	6.1%	4.5%
	MAE	4.9%	6.2%	3.9%	1.7%	2.5%	1.8%	5.0%	3.7%
	MAPE	26.1%	24.2%	14.8%	5.9%	8.9%	4.2%	11.2%	13.6%
	MADPE	29.1%	23.4%	14.8%	6.0%	9.8%	4.3%	11.4%	**14.1%**

6. Conclusions

In this work an ARIMAX and NARX models for solar and wind energy generation forecasting have been developed. The model is developed to obtain hourly results for one day-ahead or main market, from +12 to +36h. Both of the proposed models accept as inputs the time series to forecast and explanatory time series to improve the accuracy of the results. In the case of solar power the explanatory variable used is the irradiation; for wind power the explanatory variable used is the wind speed.

Once the forecasts are compared with the error figures, the results point out that the proposed NARX method outperform ARIMAX for both generation forecasts. It also points out that solar forecasts are more accurate that wind forecasts.

Nevertheless, the solar generation results are very tight for ARIMAX and NARX methods. RMSE, MAE and MAPE values are practically the same and it only differs slightly for MADPE when NARX method (13.51%) outperforms ARIMAX method (15.98%). This indicator is the most reliable for generations which fall off to values close to 0MWh as the solar generation does during the night.

For wind generation the results are much clearer. NARX method outperforms ARIMAX in every single error figure. In terms of MAPE, the result for NARX is 13.62% and ARIMAX reaches 21.67%. MADPE values are similar to MAPE in this case.

The results of performance achieved with NARX method for solar and wind forecasts in terms of MADPE are very similar; 13.51% in solar and 14.12% in wind. On the other hand the results obtained with the ARIMAX method in terms of MADPE differ for solar and wind forecasts; while in solar forecast the result is similar to the achieved in NARX, 15.98%; the results in wind generation are much worse reaching 22.77%, which is the worst result obtained for any of the proposed forecasting methods.

MBE figure shows the trend of the error in forecasting, if it is either overestimated or it is a lower value of energy generation. When averaging this figure on weekly basis the absolute value tends to decrease since the errors cancel themselves.

7. Acknowledgements

This work is supported by the European Union under FP7 grant contract 'Solar Heat Integration Network' (SHINE) and the fellowship at Sampol Ingeniería y Obras S.A. (317085) in the framework of Marie-Curie initial research training network (ITN).

8. References

Astariz, S., Perez-Collazo, C., Abanades, J., Iglesias, G., 2015. Towards the optimal design of a co-located wind-wave farm. Energy 84, 15–24. doi:10.1016/j.energy.2015.01.114

Benghanem, M., 2011. Optimization of tilt angle for solar panel: Case study for Madinah, Saudi Arabia. Appl. Energy 88, 1427–1433. doi:10.1016/j.apenergy.2010.10.001

Biga, A.J., Rosa, R., 1980. Estimating solar irradiation sums from sunshine and cloudiness observations. Sol. Energy. doi:10.1016/0038-092X(80)90334-5

Cassola, F., Burlando, M., 2012. Wind speed and wind energy forecast through Kalman filtering of Numerical Weather Prediction model output. Appl. Energy 99, 154–166. doi:10.1016/j.apenergy.2012.03.054

Chen, C., Duan, S., Cai, T., Liu, B., 2011. Online 24-h solar power forecasting based on weather type classification using artificial neural network. Sol. Energy 85, 2856–2870. doi:10.1016/j.solener.2011.08.027

Da Silva Fonseca, J.G., Oozeki, T., Takashima, T., Koshimizu, G., Uchida, Y., Ogimoto, K., 2012. Use of support vector regression and numerically predicted cloudiness to forecast power output of a photovoltaic power plant in Kitakyushu, Japan. Prog. Photovoltaics Res. Appl. 20, 874–882. doi:10.1002/pip.1152

Dong, Z., Yang, D., Reindl, T., Walsh, W.M., 2013. Short-term solar irradiance forecasting using exponential smoothing state space model. Energy 55, 1104–1113. doi:10.1016/j.energy.2013.04.027

Duffie, J. a., Beckman, W. a., 2013. Solar Engineering of Thermal Processes: Fourth Edition, Solar Engineering of Thermal Processes: Fourth Edition. doi:10.1002/9781118671603

Erdem, E., Shi, J., 2011. ARMA based approaches for forecasting the tuple of wind speed and direction. Appl. Energy 88, 1405–1414. doi:10.1016/j.apenergy.2010.10.031

Huang, R., Huang, T., Gadh, R., Li, N., 2012. Solar generation prediction using the ARMA model in a laboratory-level micro-grid, in: 2012 IEEE 3rd International Conference on Smart Grid

Communications, SmartGridComm 2012. pp. 528–533. doi:10.1109/SmartGridComm.2012.6486039

Lange, M., Focken, U., 2006. Physical approach to short-term wind power prediction, Physical Approach to Short-Term Wind Power Prediction. Springer Berlin Heidelberg. doi:10.1007/3-540-31106-8

Li, G., Shi, J., 2010. On comparing three artificial neural networks for wind speed forecasting. Appl. Energy 87, 2313–2320. doi:10.1016/j.apenergy.2009.12.013

Liu, H., Shi, J., Qu, X., 2013. Empirical investigation on using wind speed volatility to estimate the operation probability and power output of wind turbines. Energy Convers. Manag. 67, 8–17. doi:10.1016/j.enconman.2012.10.016

Lorenz, E., Hurka, J., Heinemann, D., Beyer, H.G., 2009. Irradiance forecasting for the power prediction of grid-connected photovoltaic systems. IEEE J. Sel. Top. Appl. Earth Obs. Remote Sens. 2, 2–10. doi:10.1109/JSTARS.2009.2020300

Mahoney, W.P., Parks, K., Wiener, G., Liu, Y., Myers, W.L., Sun, J., Delle Monache, L., Hopson, T., Johnson, D., Haupt, S.E., 2012. A Wind Power Forecasting System to Optimize Grid Integration. IEEE Trans. Sustain. Energy. doi:10.1109/TSTE.2012.2201758

Mellit, A., Pavan, A.M., 2010. A 24-h forecast of solar irradiance using artificial neural network: Application for performance prediction of a grid-connected PV plant at Trieste, Italy. Sol. Energy 84, 807–821.

Monteiro, C., Fernandez-Jimenez, L.A., Ramirez-Rosado, I.J., Muñoz-Jimenez, A., Lara-Santillan, P.M., 2013a. Short-term forecasting models for photovoltaic plants: Analytical versus soft-computing techniques. Math. Probl. Eng. 2013. doi:10.1155/2013/767284

Monteiro, C., Santos, T., Fernandez-Jimenez, L.A., Ramirez-Rosado, I.J., Terreros-Olarte, M.S., 2013b. Short-term power forecasting model for photovoltaic plants based on historical similarity. Energies 6, 2624–2643. doi:10.3390/en6052624

Paulescu, M., Badescu, V., Brabec, M., 2013. Tools for PV (photovoltaic) plant operators: Nowcasting of passing clouds. Energy 54, 104–112. doi:10.1016/j.energy.2013.03.005

Perez-Mora, N., Canals, V., Martinez-Moll, V., 2015. Short-Term Spanish Aggregated Solar Energy Forecast. Springer-Verlag Berlin Heidelberg 2011, Palma de Mallorca, pp. 307–319. doi:10.1007/978-3-319-19222-2_26

Perez-Mora, N., Martinez-Moll, V., Canals, V., 2016. DHC load management using demand forecast. Energy Procedia 91, 557–566. doi:10.1016/j.egypro.2016.06.198

Qazi, A., Fayaz, H., Wadi, a., Raj, R.G., Rahim, N. a., 2015. The artificial neural network for solar radiation prediction and designing solar systems: a systematic literature review. J. Clean. Prod. 104, 1–12. doi:10.1016/j.jclepro.2015.04.041

Reikard, G., 2009. Predicting solar radiation at high resolutions: A comparison of time series forecasts. Sol. Energy 83, 342–349. doi:10.1016/j.solener.2008.08.007

Rubin, O.D., Babcock, B. a., 2013. The impact of expansion of wind power capacity and pricing methods on the efficiency of deregulated electricity markets. Energy 59, 676–688. doi:10.1016/j.energy.2013.07.020

Sharma, N., Sharma, P., Irwin, D., Shenoy, P., 2011. Predicting solar generation from weather forecasts using machine learning, in: 2011 IEEE International Conference on Smart Grid Communications, SmartGridComm 2011. pp. 528–533. doi:10.1109/SmartGridComm.2011.6102379

Sørensen, P., Hansen, A.D., Rosas, P.A.C., 2002. Wind models for simulation of power fluctuations from wind farms. J. Wind Eng. Ind. Aerodyn. 90, 1381–1402. doi:10.1016/S0167-6105(02)00260-X

Sulaiman, S.., Rahman, T.. A., Musirin, I., 2009. Partial Evolutionary ANN for Output Prediction of a Grid-Connected Photovoltaic System. Int. J. Comput. Electr. Eng. 1, 40–45. doi:10.7763/IJCEE.2009.V1.7

Tseng, F.-M., Yu, H.-C., Tzeng, G.-H., 2002. Combining neural network model with seasonal time series ARIMA model. Technol. Forecast. Soc. Change 69, 71–87. doi:10.1016/S0040-1625(00)00113-X

Y. Gala, A. Fernández, J. Dorronsoro, 2014. Machine Learning Prediction of Global Photovoltaic Energy in Spain, in: International Conference on Renewable Energies and Power Quality (ICREPQ'14). Springer Verlag, Cordoba (Spain).

Yang, D., Jirutitijaroen, P., Walsh, W.M., 2012. Hourly solar irradiance time series forecasting using cloud cover index. Sol. Energy 86, 3531–3543. doi:10.1016/j.solener.2012.07.029

Zhang, Y., Wistar, S., Piedra-Fernandez, J.A., Li, J., Steinberg, M.A., Wang, J.Z., 2014. Locating visual storm signatures from satellite images, in: 2014 IEEE International Conference on Big Data (Big Data). pp. 711–720. doi:10.1109/BigData.2014.7004295